Supplementary Information

Identification of parvalbumin interneurons as cellular substrate of fear memory persistence

Gürsel Çalışkan[1,2,*], Iris Müller[2,*], Marcus Semtner[3], Aline Winkelmann[3,4], Ahsan S. Raza[2], Jan O. Hollnagel[1,5], Anton Rösler[1], Uwe Heinemann[1], Oliver Stork[2,6,$] and Jochen C. Meier[3,4,$]

[1] Institute for Neurophysiology, Charité Universitätsmedizin Berlin, 14195 Berlin, Germany
[2] Institute of Biology, Department of Genetics & Molecular Neurobiology, Otto-von-Guericke-University, 39120 Magdeburg, Germany
[3] Zoological Institute, Division Cell Physiology, 38106 Braunschweig, Germany
[4] RNA editing and Hyperexcitability Disorders Helmholtz Group, Max Delbrück Center for Molecular Medicine in the Helmholtz Association, 13125 Berlin, Germany
[5] Institute of Physiology and Pathophysiology, University of Heidelberg, 69120 Heidelberg, Germany
[6] Center for Behavioral Brain Sciences, Magdeburg, Germany

[*,$] Equal contribution

Correspondence:

Prof. Dr. Jochen C. Meier
Zoological Institute, Division Cell Physiology
Spielmannstr. 7
38106 Braunschweig
Germany
Phone: +49-(0)531-391 3254
Email: jochen.meier@tu-braunschweig.de

Supplementary Methods

Behavior

Before experiments all animals were single caged and handled extensively. First, mice were tested in the hot plate test to rule out *a priori* differences in pain sensitivity. Mice were placed on a 55 °C hot plate and their latency to lick hind paws was assessed by an experimenter who was blind with respect to the animal genotype. Immediately after first occurrence or after a maximum duration of 30 s, mice were removed from the plate to avoid tissue damage (Wrenn et al., 2004).

19 days later fear conditioning and extinction training took place in a sound isolation cubicle containing a 16 x 32 x 20 cm acrylic glass arena with a grid floor, loudspeaker and ventilation fan (background noise 70 dB SPL, light intensity < 10 lux; TSE, Bad Homburg, Germany). Three training sessions were applied on consecutive days, each comprising 2 min initial context exposure followed by mild electric foot shock (1 s, 0.4 mA) and additional 30 s in the training apparatus. One day after the last training, extinction training commenced with five daily 10 min exposures to the training context without any foot shock reinforcement. Freezing behavior (lack of any detectable movement except for respiration) was determined as a measure of fear. Data were analyzed in 2 min bins throughout training and extinction to isolate possible time-dependent between-session and within-session effects in a most accurate manner possible. Data is reported as percent time of the investigated 2 min time interval (except Suppl. Figure 6). The first 2 min of each training and extinction session were taken for the analysis of long term memory; moreover, planned comparison of the last 2 min interval with the first interval of the following extinction session was done to determine fear recovery between two sessions. Animal behavior was assessed online via a photo beam detection system and the number of freezing bouts > 1 s and the total duration of freezing behavior were assessed as established measures of fear memory (Albrecht et al., 2013;

Laxmi et al., 2003). Baseline activity levels were evaluated before first shock application (with activity defined as time spent moving at a velocity between 3 to 20 cm/s).

To investigate whether the observed deficit is specific for contextual fear memory or more generally related to deficits in fear extinction, we performed auditory cued fear conditioning and extinction in a separate batch of *Hprt*$^{\alpha 3L185L\ +/0}$; *Pvalb*$^{Cre\ +/-}$ mice (N = 10) and *Hprt*$^{\alpha 3L185L\ +/0}$ control mice (N = 9). As described before mice were single caged before the experiment started. Before conditioning, animals were adapted to the chamber twice a day on two consecutive days for 6 minutes per session. On the third day, mice were trained with three tone/shock pairings (tone: 9 s, 10 kHz, 85 dB SPL co-terminating with a foot shock: 1 s, 0.4 mA; ISI: 20 s), preceded and followed by each 2 min without acoustic stimulus presentation. For the next five days, mice received extinction training for the cue in the neutral context (a standard home cage, placed into the training apparatus; R/E1-E5). One extinction session consisted of a total of 20 tone presentations (each 10 s) with ISI of each 20 s and was again preceded and followed by 2 min without acoustic stimulus presentation. In addition to a stimulus-by-stimulus analysis, to allow for comparison to contextual extinction, auditory fear memory was assessed in 2 min bins throughout training and extinction. Data is reported as percent time of the investigated 2 min time interval. For tone-specific fear memory, freezing duration and number of freezing bouts during the first 4 CS presentations were averaged and used for analysis. Finally, after extinction training the cue was presented in the original shock context to test for context-induced fear renewal (Fig. 3).

Electrophysiology

In total, 18 naïve control mice (*Hprt*$^{\alpha 3L185L\ +/0}$; n = 64 slices) and 16 *Hprt*$^{\alpha 3L185L\ +/0}$; *Pvalb*$^{Cre\ +/-}$ mice (n = 68 slices) were investigated. CA3-CA1 network interactions during SPW-R activity was investigated using 5 naïve control mice (*Hprt*$^{\alpha 3L185L\ +/0}$; n = 19 slices) and 4 *Hprt*$^{\alpha 3L185L\ +/0}$; *Pvalb*$^{Cre\ +/-}$ mice (n = 15 slices). For correlation of SPW-R activity and freezing behavior additional 8 control mice (*Hprt*$^{\alpha 3L185L\ +/0}$; n = 40 slices) and 8 *Hprt*$^{\alpha 3L185L\ +/0}$; *Pvalb*$^{Cre\ +/-}$ mice (n =

37 slices) were studied after extinction session E2. For slice preparation, mice were decapitated under N_2O (70 % N_20 - 30 % O_2) and isoflurane (starting with 3 % isoflurane and then rapidly reducing it to 0.5 %). Brains were placed in ice-cold artificial carbogenated (5% CO_2 - 95% O_2) cerebrospinal fluid (ACSF) which contained (in mM) 129 NaCl, 21 $NaHCO_3$, 3 KCl, 1.6 $CaCl_2$, 1.8 $MgSO_4$, 1.25 NaH_2PO_4 and 10 glucose, pH 7.4, osmolarity: 300 ± 5 mosm / kg. Horizontal hippocampal slices (400 µm at bregma -4.7 to -7.3 mm, 3-4 slices from most ventral portion) were prepared at an angle of 12° in the fronto-occipital direction (with the frontal portion up) using a vibratome (752 M Vibroslice, Campden Instruments). To achieve dorsal transverse-like slices, we used several methods described in the literature (Papatheodoropoulos and Kostopoulos 2000; Papatheodoropoulos and Kostopoulos 2002; Dougherty et al., 2012; Steullet et al., 2010). First, the dorsal part of the hippocampus was isolated and glued to the cutting platform, the most dorsal part facing upwards. The stability of the hippocampus during slice cutting was achieved via an agar block positioned behind the hippocampus. Second, ~30° or ~45° tilted coronal hemisphere sections were cut to obtain transverse slices of the dorsal hippocampus (Dougherty et al., 2012; Steullet et al., 2010). Last, parasagittal hemisphere sections (~30° tilted or without any angle) were cut to achieve transverse-like dorsal hippocampal slices. None of the dorsal hippocampal slices prepared using the methods described above showed any spontaneous SPW-Rs (N = 8 mice, n = 48 slices). This is in line with the previous observations showing lack of spontaneous activity in isolated dorsal hippocampal slices (Papatheodoropoulos and Kostopoulos 2002).

Brain slices were transferred to an interface recording chamber continuously perfused with ACSF at a flow rate of 1.8 ± 0.2 ml / min at 36 ± 0.1 °C. Slices were incubated for at least one hour before starting field potential (FP) recording using microelectrodes (5-10 MΩ) filled with ACSF. Signals were pre-amplified using a custom-made amplifier equipped with negative capacitance compensation and low-pass filtered at 3 kHz. Signals were sampled at a frequency of 5-10 kHz and stored on a computer hard disc for off-line analysis (Cambridge Electronic Design, Cambridge, UK).

Recordings were made in *stratum pyramidale* (SP) of CA1 and CA3. After at least one hour of slice recovery, the majority of the ventral horizontal slices exhibited spontaneous SPW-Rs in the hippocampus. For analysis of SPW-Rs, data files with 3 min recording time were extracted and further analyzed using a MATLAB-based code (MathWorks, Natick, MA). Sharp waves (SPW) were detected by low-pass filtering the data at 45 Hz. For the filtering of the recordings, an 8-order symmetric Butterworth filter was used (He et al., 2010). The threshold for event detection was set to 3 times the standard deviation added to the mean of the lowpass-filtered signal. Also, the minimal time interval between two subsequent SPW was set to 100 ms. An event crossing the threshold but closer than 80 ms to the previous SPW was discarded. Data stretches of 125 ms centered to the maximum of sharp wave event were stored for further analysis. To analyze area under the curve of SPW events points crossing the mean of the data were used as start and end point of a SPW. The area under curve was measured using trapezoidal numerical integration of low pass-filtered data.

To isolate ripples, raw data was band-pass filtered at 120-300 Hz. In our preparation, the ripples usually occurred at the ascending phase of the sharp wave. The number of ripples changed from 1 to 5 ripples per SPW. Thus data stretches of 15 ms before and 10 ms after the maximum of SPW events (25 ms) were stored for further analysis. Threshold for ripple detection was set to 3 times standard deviation of the band-pass filtered signal. To analyze the ripple amplitude, triplepoint-minimax-determination was used. If the difference between falling and rising component of a ripple was higher than 75 %, ripples were discarded from analysis. Frequencies of the ripples were calculated only from subsequent ripples. Ripple measurements in vivo are obtained from the area CA1. To our knowledge, the ripple occurrence in area CA3 in vivo is weak. SPW bursts emerges in the CA3 subregions and spread to the CA1 area in vivo. During slow wave sleep that is when hippocampal SPWs occur, the coherent discharge of a small group of CA3 cells is the primary cause of spiking activity in CA1 pyramidal neurons and ripple occurrence in the area CA1 (Csicsvari et al.,

2000). However, in slice preparations one can also observe the ripples superimposed to a slow wave (sharp wave) also in the area CA3 (Maier et al., 2003). Thus, to make a complete in depth analysis, we have also included the CA3 ripple data in our analysis.

For the definition of the noise level, the detected peak (trough) distribution was decomposed by a bivariate gaussian mixture distribution model supplied by Matlab's statistics toolbox (gmddistribution class). The aim was to define the most prominent distribution part of small noise values which is assumed to follow a gaussian distribution. This was confirmed by visual inspection.

From the estimated noise distribution parameters (mean and standard deviation) a set of confidence levels were tested, starting from 2 up to 20 standard deviations above the mean in four hundred steps. The test variable, here called peak signal-to-noise ratio, was defined as ratio of the squared mean peak value of the fraction above the tested confidence level (power of signal - SPW peak) to the squared mean peak value of the fraction below the tested confidence level (power of signal without SPW). If the tested confidence level reached the values close to the large amplitude values of the SPW events, a large increase of the peak signal-to-noise ratio followed. In order to detect prominent changes of the peak signal-to-noise ratio in dependence of the tested confidence levels, a reference line was defined. The reference line begins at the test function value of the smallest tested confidence level and ends at the test function value of the highest tested confidence level. The finally used confidence level was set at the largest deviation from the reference line.

Only those peak values were accepted that were above the confidence level of the noise distribution. For parameter estimation (mean and standard deviation) of the peak value distributions a gaussian distribution fitting procedure was applied (normpdf supplied by matlab's statistics toolbox). For parameter (shape and scaling parameter) estimation of the inter-event interval distributions a gamma distribution fitting procedure was applied (gamfit

supplied by matlab's statistics toolbox). Events following their predecessors within less than 100 ms were discarded.

For analysis of SPW propagation from CA3 to CA1, the temporal relationship between presumably connected SPW events between CA3 (starter) and CA1 (follower) was analyzed. The connected SPW events had to fulfil the following criteria: 1) A follower event occurred between two successive starter event times (larger or equal: the first starter event time; smaller: the subsequent starter event time). If there were more than one follower event detected, only the closest one was used to calculate the temporal relationship. 2) The distributions of the time distance of the connected events were quantified, and connected events were included if their time distance were below the 0.05 level of the cumulative density function of the time distance distribution. Event trains were created with the sampling period of the recording. Each accepted event time was set to one (else zero). Such an event train was convolved by a gaussian function with a standard deviation of 2 ms (95 % of the area within the duration of 8 ms). For both, the global detected event times and the defined connected event times of the two areas, the respective event trains were cross correlated (lag zero normalized). The analyzed lag range was +/- 30 ms. The cross-correlation function was analyzed by detecting the global maximum correlation value and its lag time. Furthermore, the peak values of the connected events were correlated (the zero lag of the normalized covariance function). All value distributions were Box-Cox transformed if they did not satisfy the Lilliefors test (alpha=5 %).

Correlation between SPW-R activity and freezing behavior

Animals were sacrificed 1 h after the extinction session E2, and horizontal slices were obtained from the ventral hippocampus as described above. Per mouse 6-8 slices were obtained and SPW-Rs were recorded simultaneously during 10 min from areas CA3 and CA1. Only slices exhibiting SPW-Rs in both CA3 and CA1 were further processed for correlation analysis (2-5 slices per mouse). Propagation failure, CA1 incidence, CA3-CA1

correlation, CA3 signal-to-noise ratio, and CA3-CA1 latency were extracted from each slice. The average value per mouse was obtained by averaging the values obtained from each slice. This value was further used for analysis of correlation with freezing duration (in percent time of 2 min) at E2.

References

Albrecht A, Caliskan G, Oitzl MS, Heinemann U, Stork O. 2013. Long-lasting increase of corticosterone after fear memory reactivation: anxiolytic effects and network activity modulation in the ventral hippocampus. Neuropsychopharmacology. 38:386-394.

Csicsvari J, Hirase H, Mamiya A, Buzsaki G. 2000. Ensemble patterns of hippocampal CA3-CA1 neurons during sharp wave-associated population events. Neuron. 28:585-594.

Dougherty KA, Islam T, Johnston D. 2012. Intrinsic excitability of CA1 pyramidal neurones from the rat dorsal and ventral hippocampus. J Physiol. 590:5707-5722.

He BJ, Zempel JM, Snyder AZ, Raichle ME. 2010. The temporal structures and functional significance of scale-free brain activity. Neuron. 66:353-369.

Laxmi TR, Stork O, Pape HC. 2003. Generalisation of conditioned fear and its behavioural expression in mice. Behav Brain Res. 145:89-98.

Maier N, Nimmrich V, Draguhn A. 2003. Cellular and network mechanisms underlying spontaneous sharp wave-ripple complexes in mouse hippocampal slices. J Physiol. 550:873-887.

Papatheodoropoulos C, Kostopoulos G. 2000. Dorsal-ventral differentiation of short-term synaptic plasticity in rat CA1 hippocampal region. Neurosci Lett. 286:57-60.

Papatheodoropoulos C, Kostopoulos G. 2002. Spontaneous, low frequency (approximately 2-3 Hz) field activity generated in rat ventral hippocampal slices perfused with normal medium. Brain Res Bull. 57:187-193.

Steullet P, Cabungcal JH, Kulak A, Kraftsik R, Chen Y, Dalton TP, *et al*. 2010. Redox dysregulation affects the ventral but not dorsal hippocampus: impairment of parvalbumin neurons, gamma oscillations, and related behaviors. J Neurosci. 30:2547-2558.

Wrenn CC, Kinney JW, Marriott LK, Holmes A, Harris AP, Saavedra MC, *et al*. 2004. Learning and memory performance in mice lacking the GAL-R1 subtype of galanin receptor. Eur J Neurosci. 19:1384-1396.

SUPPLEMENTARY FIGURE 1. Acquisition and filtering of the SPW-R data from horizontal ventral hippocampal slice preparations. **(A)** Sketch of a hippocampus illustrating the positioning of the electrodes. Note that the electrodes were positioned at pyramidal cell layers of CA3 and CA1. **(B)** Example of a sharp-wave ripple (SPW-R, top); traces of ripple oscillations (middle) and SPW (bottom) of the same SPW-R. The data were recorded at 5 or 10 kHz. The slow component (SPW) was obtained by low-pass filtering at 45 Hz while the ripple component was obtained by band-pass filtering between 120 and 300 Hz.

SUPPLEMENTARY FIGURE 2. Lack of correlation between background fluorescence in ventral hippocampal slices and freezing duration. **(A)** Background fluorescence in relation to laser power. Each slice processed for confocal microscopy is represented by a circle. Control and *Hprt*$^{\alpha 3L185L\ +/0}$; *Pvalb*$^{Cre\ +/-}$ mice are color coded grey and blue, respectively. **(B)** Freezing duration (in percent time of 2 min) at E2 in relation to background fluorescence. Animals are represented using grey and blue circles.

SUPPLEMENTARY FIGURE 3. Over-night return of fear memory after extinction. All genotypes displayed comparable freezing levels in the last 2 min of each session. However, while freezing levels were maintained at comparable levels in *Hprt*$^{\alpha 3L185L\ +/0}$ and *Hprt*$^{\alpha 3L185L\ +/0}$; *Camk2a*$^{Cre\ +/-}$ mice, they significantly increased in *Hprt*$^{\alpha 3L185L\ +/0}$; *Pvalb*$^{Cre\ +/-}$ mice in the first 2 min period of the subsequent session. Data represent mean +/- SEM. R = retrieval, E1-5 = extinction days 1-5. Significant difference between subsequent extinction sessions within a genotype for *Hprt*$^{\alpha 3L185L\ +/0}$; *Pvalb*$^{Cre\ +/-}$ mice is indicated using & or && symbols (&: $p < 0.05$; &&: $p < 0.01$).

SUPPLEMENTARY FIGURE 4. Sharp wave-ripples (SPW-Rs) in area CA1 of *Hprt*$^{\alpha 3L185L\ +/0}$; *Pvalb*$^{Cre\ +/-}$ mutant mice. **(A)** Example traces of SPW-Rs recorded in pyramidal cell layer of CA1 in ventral horizontal hippocampal slice preparations. **(B)** Representative traces of SPW-

R (top trace), ripples (middle trace) and SPW (bottom trace) of each genotype. For values see Table 1.

SUPPLEMENTARY FIGURE 5. Pearson product-moment correlation coefficient "R" was used to assess correlation between freezing duration at E2 and SPW-R properties. Freezing duration at E2 negatively correlates with CA3-CA1 event failure (**A**, R = - 0.536; *: $p < 0.05$) and positively correlates with CA1 SPW incidence (**B**, R = 0.538; *: $p < 0.05$).

SUPPLEMENTARY FIGURE 6. Pearson product-moment correlation coefficient "R" was used to assess correlation between freezing duration in seconds at E2 and mean percentage of neurons with different PV signal intensities classified according to the four different PV signal intensity groups. In area CA3b of the ventral hippocampus, freezing duration at E2 positively correlated across genotypes with mean percentages of PV interneurons classified "intermediate high" (**A**, R = 0.59, *: $p < 0.05$), while it negatively correlated with mean percentages of PV interneurons classified "low" (**A**, R = -0.74, **: $p < 0.01$). In the dorsal hippocampus **(B)**, freezing duration at E2 did not correlate with any of the four fractions of PV interneurons. Grey and blue colored circles identify control and *Hprt*$^{\alpha 3L185L\ +/0}$; *Pvalb*$^{Cre\ +/-}$ mice, respectively.

Suppl. Figure 1

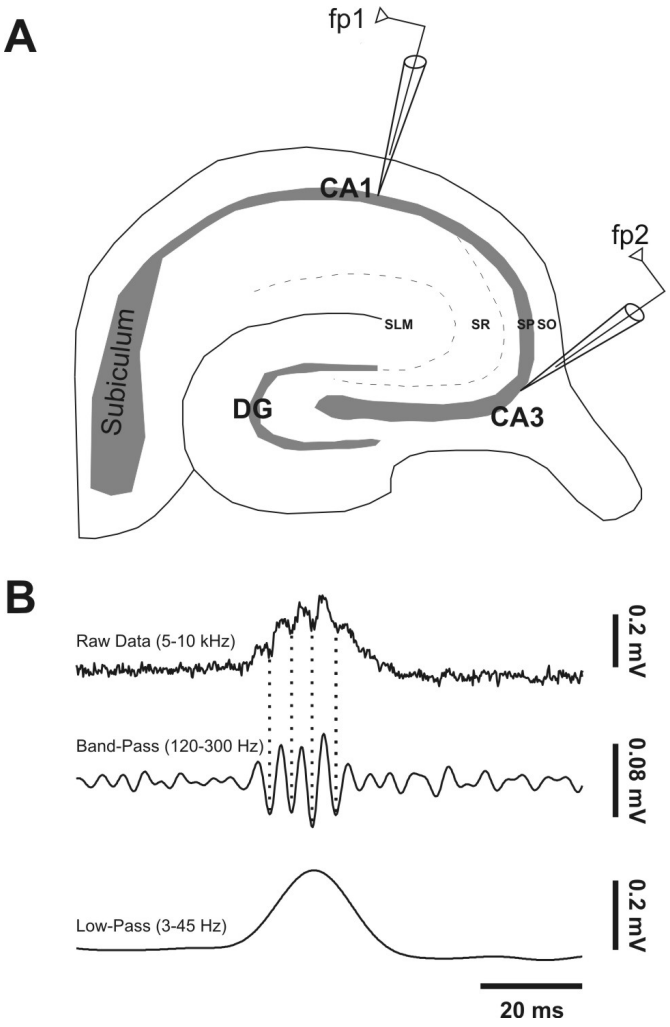

Suppl. Figure 2

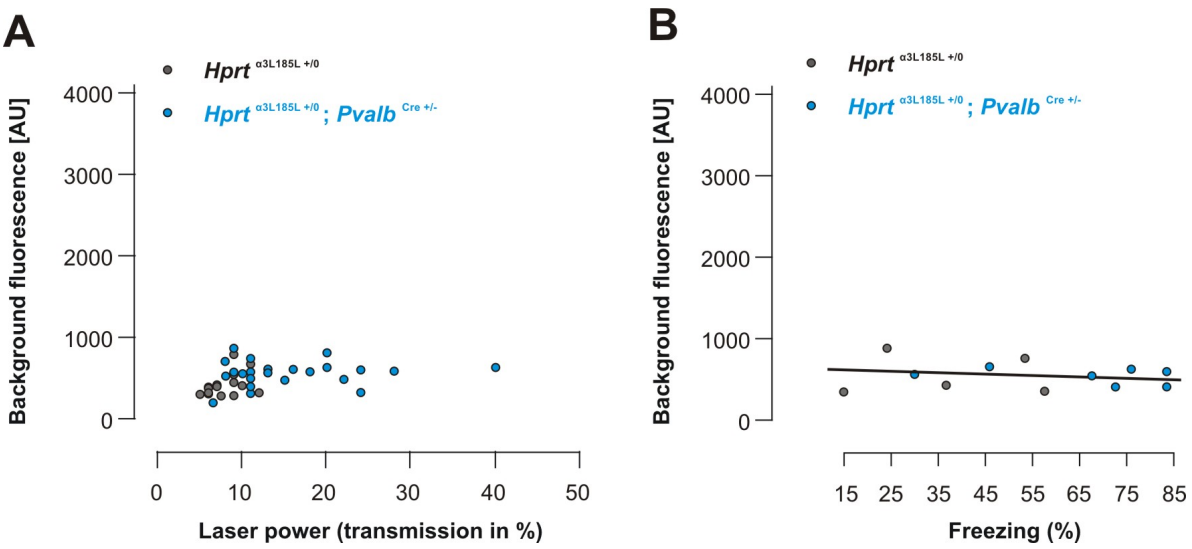

Suppl. Figure 3

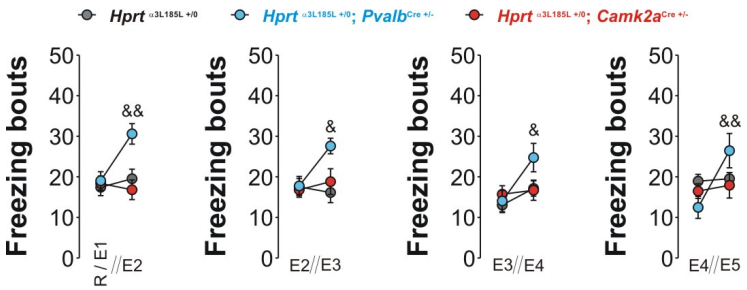

Suppl. Figure 4

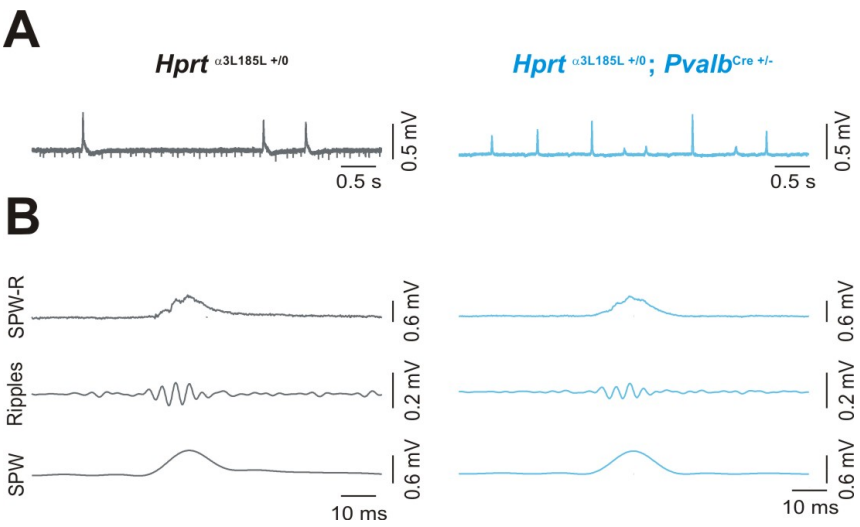

Suppl. Figure 5

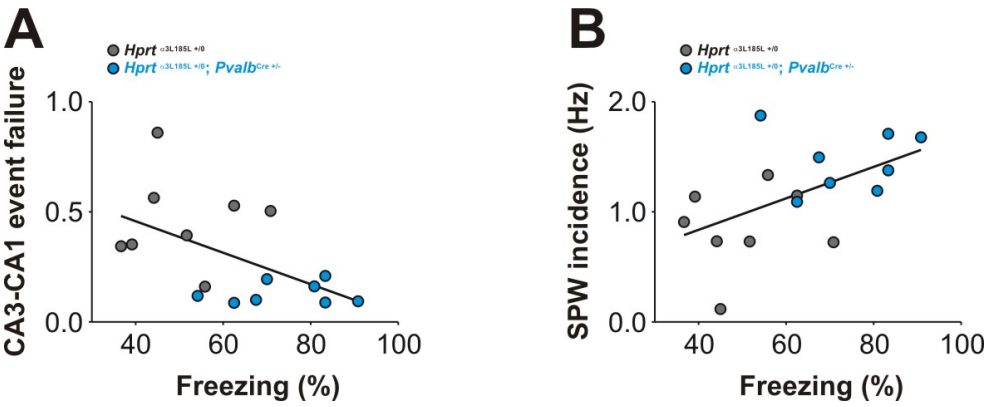

Suppl. Figure 6